# Wildland–urban interface wildfire increases metal contributions to stormwater runoff in Paradise, California

**Article** *in* Environmental Science: Processes and Impacts · February 2024

DOI: 10.1039/d3em00298e

CITATIONS
5

READS
284

**12 authors**, including:

Lauren J. Magliozzi
University of Colorado Boulder
**3** PUBLICATIONS **6** CITATIONS
SEE PROFILE

Sandrine J. Matiasek
California State University, Chico
**13** PUBLICATIONS **357** CITATIONS
SEE PROFILE

Charles N Alpers
United States Geological Survey
**202** PUBLICATIONS **7,599** CITATIONS
SEE PROFILE

Julie Korak
University of Colorado Boulder
**36** PUBLICATIONS **1,305** CITATIONS
SEE PROFILE

Volume 26
Number 4
April 2024
Pages 647–794

# Environmental Science
## Processes & Impacts

rsc.li/espi

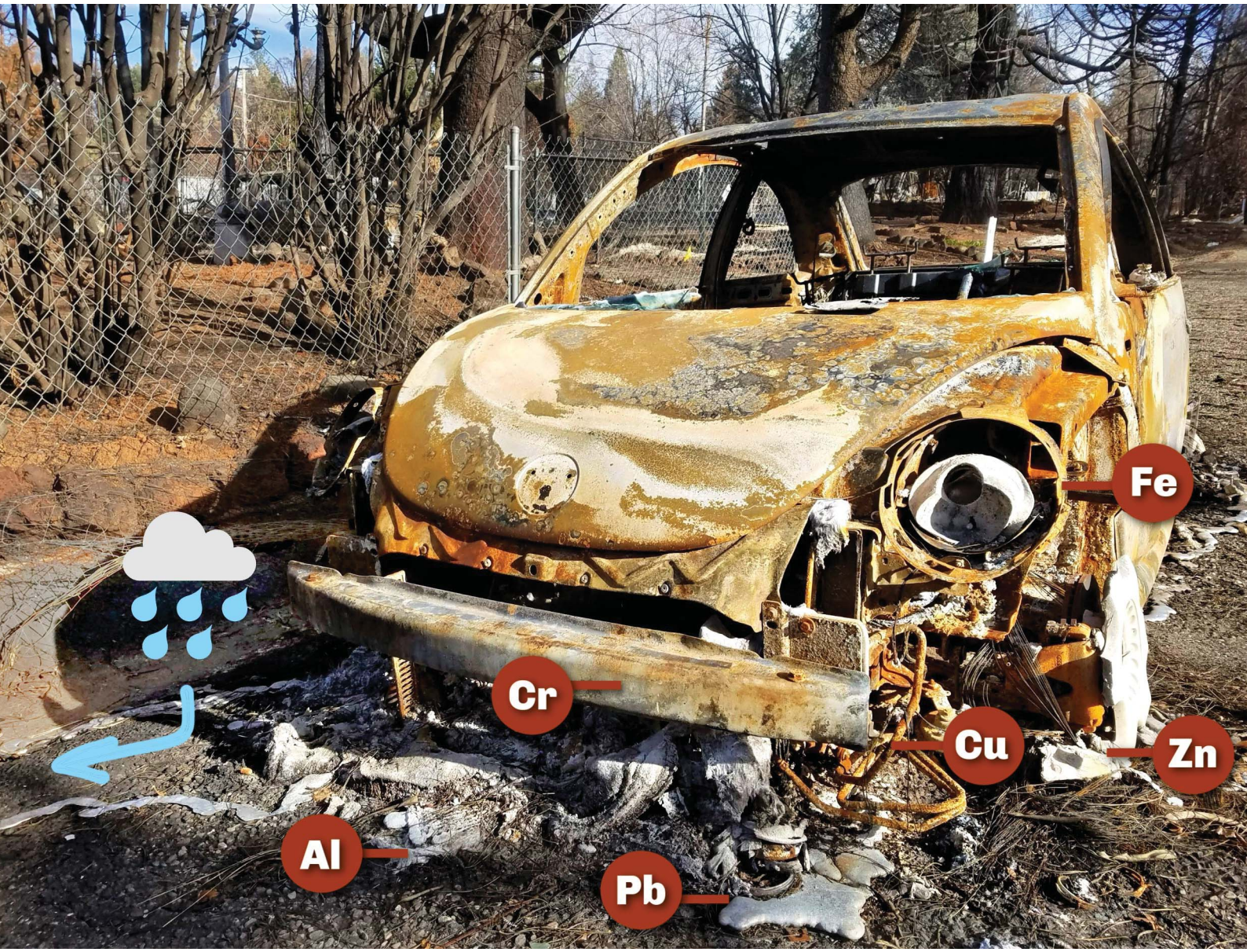


ISSN 2050-7887

ROYAL SOCIETY OF CHEMISTRY

**PAPER**
Jackson P. Webster *et al.*
Wildland–urban interface wildfire increases metal contributions to stormwater runoff in Paradise, California

Environmental Science Processes & Impacts

PAPER

View Article Online
View Journal | View Issue



Cite this: *Environ. Sci.: Processes Impacts*, 2024, **26**, 667

# Wildland–urban interface wildfire increases metal contributions to stormwater runoff in Paradise, California†

Lauren J. Magliozzi, [a] Sandrine J. Matiasek, [b] Charles N. Alpers, [c] Julie A. Korak, [a] Diane McKnight, [a] Andrea L. Foster, [d] Joseph N. Ryan, [a] David A. Roth, [e] Peijia Ku, [f] Martin Tsz-Ki Tsui, [g] Alex T. Chow [h] and Jackson P. Webster *[i]

The 2018 Camp Fire was a large late-year (November) wildfire that produced an urban firestorm in the Town of Paradise, California, USA, and destroyed more than 18 000 structures. Runoff from burned wildland areas is known to contain ash, which can transport contaminants including metals into nearby watersheds. However, due to historically infrequent occurrences, the effect of wildland-urban interface (WUI) fires, such as the Camp Fire, on surface water quality has not been well-characterized. Therefore, this study investigated the effects of widespread urban burning on surface water quality in major watersheds of the Camp Fire area. Between November 2018 and May 2019, 140 surface water samples were collected, including baseflow and stormflow, from burned and unburned watersheds with varying extent of urban development. Samples were analyzed for total and filter-passing metals, dissolved organic carbon, major anions, and total suspended solids. Ash and debris from the Camp Fire contributed metals to downstream watersheds *via* runoff throughout the storm season. Increases in concentration up to 200-fold were found for metals Cr, Cu, Ni, Pb, and Zn in burned watersheds compared to pre-fire values. Total concentrations of Al, Cd, Cu, Pb, and Zn exceeded EPA aquatic habitat acute criteria by up to 16-fold for up to five months after the fire. To assess possible transport mechanisms and bioavailability, a subset of 18 samples was analyzed using four filters with nominal pore sizes ranging from 0.22 to 1.2 μm to determine the particulate size distribution of metals. Trace and major metals (Al, Ba, Co, Cr, Cu, Fe, Hg, Mn, Ni, Pb, and Zn) were found mostly associated with larger grain sizes (>0.45 μm), and some metals (Al, Cr, Fe, and Pb) also included a substantial colloidal phase (0.22 to 0.45 μm). This study suggests that fires in the wildland–urban interface increase metal concentrations, mainly through particulate driven transport. The metals with the largest increases are likely from anthropogenic disaster materials, though biomass ash also is a major contributor to water quality. The increase in metals following WUI burning may have adverse ecological impacts.

Received 12th July 2023
Accepted 25th January 2024

DOI: 10.1039/d3em00298e

rsc.li/espi



## Environmental significance

Wildfires that occur in forest and grassland landscapes are increasing in frequency and intensity and are escalating the risk of burning at the wildland–urban interface (WUI). The effects of wildfires in the WUI include loss of lives and livelihood, destruction of infrastructure, and long-term impacts to ecosystems. Furthermore, fires that occur in the WUI may cause potential human or ecological health issues through toxic metal contamination of surface waters in addition to smoke inhalation risk.

[a]*Environmental Engineering Program, University of Colorado Boulder, CO, USA*
[b]*Department of Earth and Environmental Sciences, California State University Chico, CA, USA*
[c]*U.S. Geological Survey, California Water Science Center, Sacramento, CA, USA*
[d]*U.S. Geological Survey, Geology, Minerals, Energy, and Geophysics Science Center, Menlo Park, CA, USA*
[e]*U.S. Geological Survey, Water Mission Area, Boulder, CO, USA*
[f]*Environmental Sciences Division, Oak Ridge National Laboratory, TN, USA*
[g]*School of Life Sciences, State Key Laboratory of Agrobiotechnology, The Chinese University of Hong Kong, Hong Kong*
[h]*Department of Forestry and Environmental Conservation, Clemson University, SC, USA*
[i]*Department of Civil Engineering, California State University Chico, CA, USA. E-mail: jwebster13@csuchico.edu*

† Electronic supplementary information (ESI) available. See DOI: https://doi.org/10.1039/d3em00298e

## 1. Introduction

The Camp Fire was the deadliest, most destructive, and most expensive wildfire in California history, and one of the costliest disasters in the world.[1] The fire killed 85 people and destroyed 18 804 structures across three communities (Paradise, Concow, and Magalia; Fig. 1), resulting in an estimated $13 billion in losses and $3 billion for cleanup.[2] Ignited by high-voltage power lines on November 8, 2018, the fire started near Pulga in the Feather River Canyon, east of the Town of Paradise and spread west due to high winds (80 km $h^{-1}$).[2] Due to the wind carrying embers that sparked new ignitions downwind (*i.e.*, firebrands), the Town of Paradise was consumed by fire within three and a half hours, resulting in an urban firestorm.[2] In contrast to wildland fires, fires at the wildland-urban interface (WUI), such as the Camp Fire, combust anthropogenic materials that may negatively impact surface water quality through runoff.

Fires in wildland areas (non-urban) are historically more common and have been the focus of most research thus far. In vegetated watersheds, runoff after wildfires alters watershed processes causing adverse impacts to surface water quality.[3] Because of increased soil hydrophobicity, rain mobilizes ash, soil, and charred materials, changing water chemistry (*e.g.*, pH and ionic composition) and increasing sediment transport, which in turn facilitates the mobilization of metals associated with sediment.[4–7] In wildland areas, mobilized metals can originate from a variety of sources, such as burned biomass, disturbed underlying geology, and isolated mining and manufacturing sites (historical or current).[5,8–10] Elevated temperatures during combustion can alter metal speciation or disrupt complexes with soil organic matter, often increasing mobility in surface waters.[8,11] Notably, some metals and metallic compounds pose acute adverse human and ecosystem health effects.[12,13]

In contrast, the water quality impacts of WUI fires have not been well-characterized because of historically infrequent occurrence, but risk is expected to increase as the WUI expands due to urban development.[14] In urban fires, man-made fuels are combusted (*e.g.*, structures, vehicles, household products, and other infrastructure) creating "disaster materials", which can include asbestos fibers, man-made vitreous fibers (*e.g.*, fiberglass insulation), metal-rich particles, and particle-associated persistent organic pollutants.[15] The extent of destruction and the variety of anthropogenic source materials that could mobilize

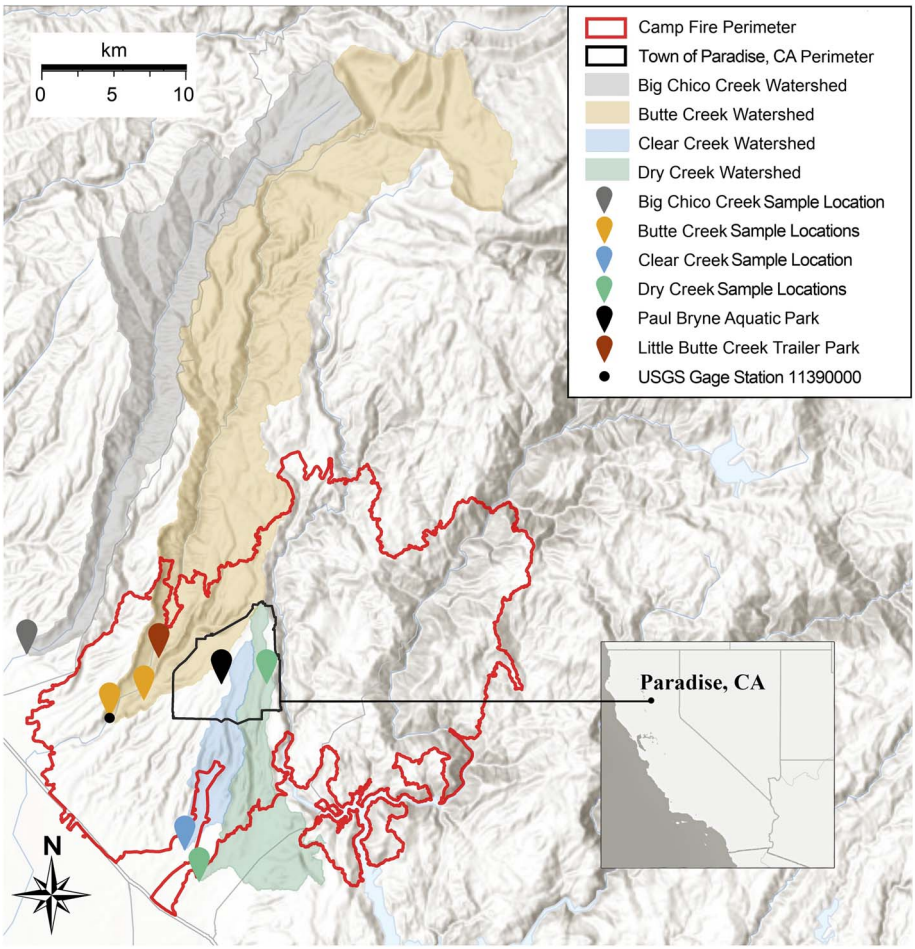


Fig. 1 Map of watersheds, sampling locations (markers) in each watershed, Town of Paradise limits (black line), and the 2018 Camp Fire perimeter (red line). The inset map displays the Town of Paradise within California. The Butte Creek stream gage is located next to the westernmost sampling point in the Butte Creek watershed. Base map produced using ArcGIS online, (ESRI, USA).

 

metals into the watershed, such as vehicles (frames, batteries, wiring, tires), structures (residential, industrial, and commercial), and structure contents (furniture, appliances, personal items) were widespread following the Camp Fire (Fig. 2).

Storm runoff can mobilize metals from disaster materials. For example, runoff collected from a simulated automobile fire conducted in the U.K. contained arsenic (As), barium (Ba), cadmium (Cd), cobalt (Co), chromium (Cr), copper (Cu), mercury (Hg), nickel (Ni), lead (Pb), and zinc (Zn).[16] In burned urban settings (London, U.K.) and on the urban fringe (California, USA), Cu, Pb, and Zn concentrations in stormwater have been found 100 to 700-fold higher compared to unburned areas.[17–20] Additionally, WUI fires are, by definition, in close proximity to populated areas, and the risk of elevated metals in stormwater runoff from these events is an emerging concern.[17,18,21,22]

Although previous work has reported elevated metal concentrations in water from WUI fires, metal speciation (*e.g.*, phase partitioning) is not well-characterized despite its importance for bioavailability and ecosystem health. At neutral pH, trace metals are commonly present in the particulate or colloidal phase, sorbed to oxides of aluminum (Al), iron (Fe), or manganese (Mn), or associated with humic substances.[23,24] Speciation is important because dissolved (filter-passing) trace metals are more readily assimilated by aquatic biota than particulate metals.[25–27] While dissolved organic matter (DOM) and trace metal mobilization may increase after a wildfire, toxicity to biota may decrease if the bioavailability of trace metals decreases due to their complexation by DOM.[5,7,28] Therefore, it is important to understand both the quantity and speciation of metals mobilized from WUI fires.


Fig. 2 Photographs of the effects of the Camp Fire taken January 2019: (a) burned vehicle from Ginny Lane in the Town of Paradise, California. (b) Little Butte Creek Trailer Park post-fire, looking east. (c) Stormwater moving through ashes of burned Little Butte Creek Trailer Park. Photo (b) at same time and location as photo c, looking west. Photo credit: J. Webster.

Because the large-scale urban destruction caused by the Camp Fire was a likely source of anthropogenic contaminants, the goal of this study was to characterize metal concentrations in surface water runoff from the burned area during storm events and baseflow conditions. We evaluated water quality parameters, such as pH, specific conductivity, total suspended solids (TSS), dissolved organic carbon (DOC), anions, and metals in the watersheds surrounding the Town of Paradise after the Camp Fire. We hypothesized that runoff would increase metal concentrations in surface waters, and that increases would be greater in watersheds with a greater extent of urban destruction. Therefore, the objective of this study was to characterize the effects of burned anthropogenic materials, such as vehicles and structures, on stormwater metal concentrations.

## 2. Methods

### 2.1. Site and watershed descriptions

Paradise (population 26 800 pre-fire) is a town located on the western slope of the Sierra Nevada and the southern Cascade Range in California (Fig. 1). The town is located on moderately sloping to level ridges surrounded by steep canyons carved by creeks that flow to the Sacramento Valley to the southwest and Lake Oroville to the southeast. The landscape is dominated by oak woodlands and grasslands southwest of town and Sierran mixed conifers at higher elevations along the northeast watershed border.

The dominant soil in the Paradise ridge is the Paradiso soil series, a loam formed on clayey residuum weathered from volcanic rock (Alfisol order, Xeralfs suborder of the USDA soil classification).[29] Clay in the surface horizon (top 10 cm) is primarily kaolinite ($Al_2Si_2O_5(OH)_4$), a highly weathered 1 : 1 non-expansive aluminosilicate clay with low cation exchange capacity, and therefore limited potential for ion exchange with metals.

Four major watersheds near the Town of Paradise were sampled (Table 1): Big Chico Creek, Butte Creek, Clear Creek, and Dry Creek (coordinates in Table S1†), which represent a variety of burn conditions and land uses. Big Chico Creek is an unburned reference watershed. Butte Creek is a semi-urban and forested watershed that was partially burned. Clear Creek and Dry Creek were both severely burned, and Clear Creek has more urban development than Dry Creek. In this context, urban refers to the areas of highest population density in this region, which do not meet the criteria for large cities.

Watershed characteristics, including elevation, land use, area, and structure damage assessment, were determined using ArcGIS (Esri, USA). Watershed area was defined as the contributing area for the sampling location. A variety of sources were used to analyze land use characteristics, number of destroyed structures, soil and bedrock geology, and historical mining activities.[30–33] There was mining in each watershed to varying degrees. Due to the presence of many small mines that were not major producers, the area of mine tailings was assumed to be a better indicator of potential water quality effects than the number of mines.

Discharge measurements were only available at the U. S. Geological Survey (USGS) Butte Creek stream gage station (USGS station 11390000), which was used to synchronize sample collection with peak stormflows for all watersheds (Fig. 3). This gage is located upstream of the western most sample location in Butte Creek (Fig. 1). During the 2018–2019 water year, precipitation in Paradise, California was approximately 1.3 times greater than the yearly average from 2010 to 2020.[34] Flows for a two-year recurrence interval were estimated with StreamStats (USGS, v4.1.1) providing the reader with a sense of relative stream sizes across watersheds.[35]

**2.1.1. Big Chico Creek.** Big Chico Creek is an unburned watershed sampled for comparison to the burned watersheds. No gaging station monitored discharge was not monitored contiuously during the 2018–19 storm season, but historical flow rates are between 0.6 $m^3\ s^{-1}$ (summer baseflow) and 170 $m^3\ s^{-1}$ (winter stormflow).[36] The watershed has lower urban land use area (1%) and a higher percentage of forested area (69%) compared to the other watersheds (Table 1). The watershed originates at 1829 m (NAVD 88) elevation and extends west for about 43 km to the Sacramento River. The upper watershed is characterized by Cascade Range basalt at high elevations and lava and mud flows from the extinct Mount Yana volcanic complex at lower elevations.[37] Vegetation transitions from Ponderosa pine (*Pinus ponderosa*) and mixed fir at high elevations to California mixed conifer and oak grasslands at lower elevations. There have been a few small fires in the watershed at low elevations, but no major fire events in the past decade. There are two historical, closed gold mines upstream, but their combined area is small (<1 $km^2$).[38]

Samples were collected at multiple locations along Big Chico Creek. Sampling occurred at the Big Chico Creek Ecological

Table 1 Characteristics of the study watersheds include watershed area in hectares, percentage of area burned in the Camp Fire, number of burned structures, percentage of urban and forested areas, percentage of mined land-use area, and number of closed gold (Au), chromium (Cr), or manganese (Mn) mines. Data sources are provided in Table S2

| Watershed | Area (hectares) | Burn area (%) | Burned structures (#) | Urban area (%) | Forest area (%) | Mined area (%) | Closed mines (#) | | |
|---|---|---|---|---|---|---|---|---|---|
| | | | | | | | Au | Cr | Mn |
| Big Chico Creek | 200 048 | 0.0 | 0 | 1.2 | 69 | 0.0 | 2 | 0 | 0 |
| Butte Creek | 40 406 | 16 | 6634 | 3.7 | 69 | 0.3 | 81 | 9 | 0 |
| Clear Creek | 3170 | 78 | 2454 | 18 | 31 | 0.0 | 0 | 0 | 0 |
| Dry Creek | 6737 | 46 | 3820 | 9.0 | 33 | 7.0 | 16 | 0 | 2 |

 

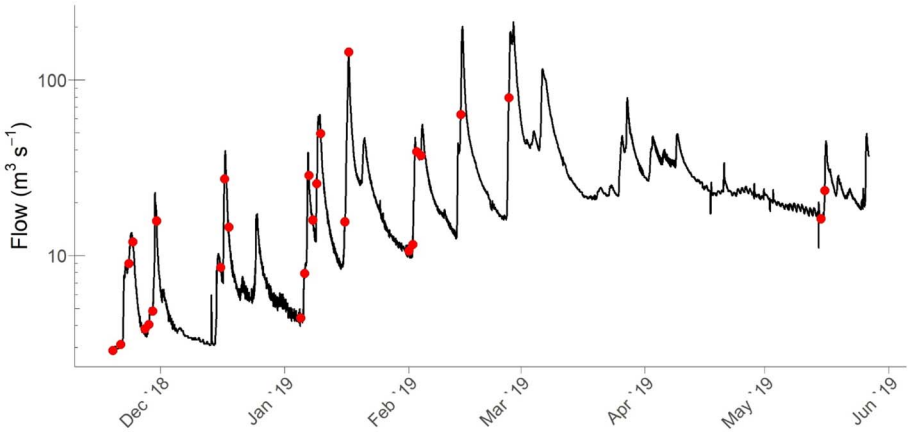


Fig. 3 Hydrograph from Butte Creek gaging station (USGS #11390000) from November 2018 to June 2019. Red dots indicate sampling events.



Reserve (15 km upstream of the City of Chico) with an autosampler when possible. Access was limited during large storms, and, on those occasions, grab samples were collected lower in the watershed, east of and 3 km upstream from the City of Chico.

**2.1.2. Butte Creek.** The Butte Creek watershed has similar characteristics to the Big Chico Creek watershed. The creeks originate within 2 km of one another and generally flow within a few kilometers of each other. Butte Creek also has low urban land use (4%) and high forested area (69%) (Table 1). In contrast to Big Chico Creek watershed, 16% of Butte Creek watershed was burned, and the watershed contains the highest number of total structures burned. Mine tailings impact about 1.2 $km^2$ of the watershed (<1%), with inactive gold mines and a small number of inactive chromium mines.[38] Discharge in Butte Creek ranged from late fall baseflow of ~2 $m^3$ $s^{-1}$ at the time of the Camp Fire to storm flows as high as 230 $m^3$ $s^{-1}$ in late February storms (Fig. 3). Like the observed maximum flows, the estimated two-year return interval stormflow is 212 $m^3$ $s^{-1}$. This similarity justifies the use of two-year return intervals to provide comparative estimates of stormflow discharges in streams that did not have stream flow measurements.

Grab samples were collected at the USGS streagage 11390000 located in the lower reach of Butte Creek Canyon (Fig. 1). When deploying an autosampler, samples were collected at the Butte Creek Ecological Preserve for increased security. These locations are 1.4 km from each other with no major water inputs or withdrawals between locations.

Little Butte Creek Trailer Park (Fig. 2b and c) was located along Little Butte Creek, a tributary of the Butte Creek watershed. All trailers and many vehicles in the park were destroyed by the fire. Storm runoff was collected from an intermittent stream draining the trailer park in January 2019 prior to site cleanup. This location represents a burned, urban end-member with direct runoff from burned anthropogenic materials.

**2.1.3. Clear Creek.** Clear Creek originates within the Town of Paradise amid residential and light commercial development. The watershed is defined by the highest percentage of total burned area (78%) and urban land use area (18%) compared to the other watersheds (Table 1). The two-year return interval stormflow is estimated at 20 $m^3$ $s^{-1}$. Sampling was conducted west of Highway 191 at Durham Pentz Road, about 14.5 km downstream of the Town of Paradise, which was initially the closest accessible location to the burned area due to prolonged evacuation orders (Fig. 1). No known mines are present in this watershed.

**2.1.4. Dry Creek.** Dry Creek also originates in the Town of Paradise. The Dry Creek watershed was 45% burned (by area) by the Camp Fire (Table 1). Dry Creek has a higher percentage of total percent forested land (33%) than total percent urban land (9%). This watershed has inactive gold and manganese mines attributing to both the largest mining-impacted area on both an absolute (total area) and relative (percent area) basis. Downstream of the fire perimeter, Dry Creek receives drainage from the Cherokee mine: a large, inactive hydraulic gold mining operation, which contributes sediment to the creek.[39] The two-year return interval stormflow is estimated to be 37 $m^3$ $s^{-1}$. Dry Creek was sampled about 17 km downstream (south) of the edge of the Town of Paradise.

**2.1.5. Paul Byrne Aquatic Park.** Grab samples were collected from an unnamed, intermittent first-order stream at Paul Byrne Aquatic Park near the south edge of the Paradise ridge, which is in the Little Dry Creek watershed. This sampling location was dominated by direct stormwater runoff during rain events. Since the Town of Paradise spans several watersheds, this sampling location represents a burned, urban end-member capturing typical anthropogenic inputs to Clear Creek from within the Town of Paradise. Samples were collected when access permitted. The two-year return interval stormflow estimate is 2 $m^3$ $s^{-1}$.

## 2.2. Sampling methods

Water samples were collected during nine storm events between November 2018 and May 2019 targeting different flow regimes including baseflow, peak storm flow, and rising and falling limbs of the stormflow hydrograph (Fig. 3). A total of 140 grab

samples were collected in new, high- or low-density polyethylene bottles that were tested for trace metal contamination using lab and field blanks. Sampling followed best practices, using nitrile-gloved hands, triple rinsing bottles with sample water prior to collection, sealing, and storing on ice until returning to the California State University Chico laboratory. During intensive storm sampling efforts, automatic samplers (Teledyne ISCO 6712) collected water in reusable, 1 L acid-washed (10% nitric acid) polypropylene bottles stored on ice. Bottles were retrieved within 24 h of sampling. In the laboratory, samples were stored at 4 °C until filtration and further processing for analyses within 48 h.

### 2.3. Water quality measurements

Prior to filtration, pH and specific conductivity were measured in well-mixed water samples at room temperature with an Oakton PCSTestr 35 handheld meter with integrated pH and specific conductivity probes, calibrated daily. Total suspended solids (TSS) were quantified by filtering a known volume of water sample (0.45 μm). Dissolved organic carbon (DOC) was measured using a high-temperature catalytic oxidation method (TOC-L, Shimadzu). Sulfate and nitrate were measured by ion chromatography (Integrion, Dionex). Elemental analysis was conducted using inductively-coupled plasma mass spectrometry (ICP-MS) (7900, Agilent). Elemental analysis included Al (aluminum), As (arsenic), Ba (barium), Ca (calcium), Cd (cadmium), Co (cobalt), Cr (chromium), Fe (iron), K (potassium), Mg (magnesium), Mn (manganese), Na (sodium), Ni (nickel), Pb (lead), Tl (thallium), Se (selenium), U (uranium), V (vanadium), and Zn (zinc). For alkali and alkaline earth elements, Ca, K, Mg, and Na are commonly observed at ppm concentrations and are collectively referred to as major cations, which excludes Ba. Important for the U.S. Environmental Protection Agency (EPA) aquatic life criteria, hardness (as mg $L^{-1}$ $CaCO_3$) was calculated using eqn S1.† Capturing differences in relative concentrations, Al, Fe, and Mn are described as major metals and remaining elements are described as trace metals. Total concentrations refer to concentrations measured in unfiltered samples. For metal, filter-passing concentrations were measured in the filtrate of a 0.45 μm cellulose nitrate filter. Total mercury (THg) was quantified on a subset of 54 samples using cold-vapor atomic fluorescence spectrometer (Model III, Brooks and Rand). Additionally, metals analysis by size fractionation within the colloidal range 0.22 μm to 1.2 μm was assessed. The grain size analysis methods and tabulated results are described in an associated USGS Data release.[40] Additional details for each analytical method are provided in the ESI.†

### 2.4. Statistical methods

Statistical analyses were performed with R Statistical Software (v4.2.1);[41] specific functions are listed in parentheses. The Shapiro test (shapiro.test()) indicated that the datasets were non-normal. We compared concentrations pre- and post-fire using the Wilcoxon *U* test (wilcox.test()) followed by the pairwise Wilcoxon *U* test (pairwise.wilcox.test()) if there were statistically significant differences. Correlations between water quality parameters were assessed using Spearman's rank correlations (ggpairs(), GGally R package v2.1.2).[42] Principal component analysis (PCA) analyzed water quality parameters in reduced space (prcomp(), stats R package v4.2.1).[41] Explanatory and response variables were standardized to have a mean of 0 and standard deviation of 1 (z-score transformation) prior to analysis. A redundancy analysis (RDA) assessed relationships between water quality and watershed characteristics, structure destruction, TSS, and flow (rda(), vegan R package v2.6.2).[43]

## 3. Results

### 3.1. Water quality comparisons

Aggregate water quality parameters were compared between watersheds to assess systematic trends, independent of temporal hydrology. The median concentrations for DOC, sulfate, and nitrate were higher in Clear Creek and Dry Creek watersheds, which had the highest number of destroyed structures per urban area (number of destroyed structures divided by area of urban land use in each watershed), compared to the unburned reference watershed. For example, the median DOC concentrations in Dry Creek and Clear Creek (4.5 mg $L^{-1}$ and 4.6 mg $L^{-1}$, respectively) were twice as high as the median DOC concentrations in Butte Creek and Big Chico Creek (1.8 mg $L^{-1}$ and 2.1 mg $L^{-1}$ respectively, Table S5†). Similarly, concentrations of sulfate, nitrate, TSS, and hardness (Fig. 4a) were statistically higher in Clear Creek and Dry Creek (Wilcoxon *U* test, $p < 0.05$, Table S9†). In all watersheds, pH values were circumneutral and ranged from 7.1 to 8.3 (Table S5†). Like DOC, sulfate, and nitrate, total concentrations of many metals (*i.e.*, Ba, Co, Cu, Pb, Ni, Mn, and Zn) were significantly greater (Wilcoxon *U*, $p < 0.05$, Table S9†) in burned watersheds compared to the unburned Big Chico Creek reference watershed (Fig. 4b, Table S11†). However, there were two exceptions. For Al and Cr, there was no statistically significant difference between Clear Creek and the unburned Big Chico Creek. In Dry Creek, the watershed with the greatest increase in median concentrations relative to unburned Big Chico Creek, Co median concentrations increased 36-fold, followed by Cu, Fe, Mn, Ni, and Pb (22- to 36-fold). Ba, Cr, Ni, and Zn median concentrations were 7- to 17-fold greater in Dry Creek compared to the reference watershed.

Little Butte Creek Trailer Park and Paul Byrne Aquatic Park (burned, urban end-members) represent sites with the greatest burned, urban impact as there was less dilution compared to the mainstem sampling locations. At these sites, total concentrations of metals were also higher than the unburned watershed and burned watersheds with more dilution. The maximum concentrations of Cu (25 μg $L^{-1}$), Pb (4.9–6.5 μg $L^{-1}$), and Zn (1100 μg $L^{-1}$) exceeded the maximum concentrations measured in mainstem sampling locations. At the Aquatic Park site, the median concentration of total Pb was higher than the other mainstem locations (4.9 μg $L^{-1}$). The maximum total Zn concentration at the Aquatic Park (256 μg $L^{-1}$) was also high compared to the mainstem locations, but the highest concentration was observed at the Little Butte Creek Trailer Park (1079 μg $L^{-1}$, Table S7†).

Throughout the 2019 water year, the highest concentrations of total (unfiltered) and filter-passing metals were observed near

 

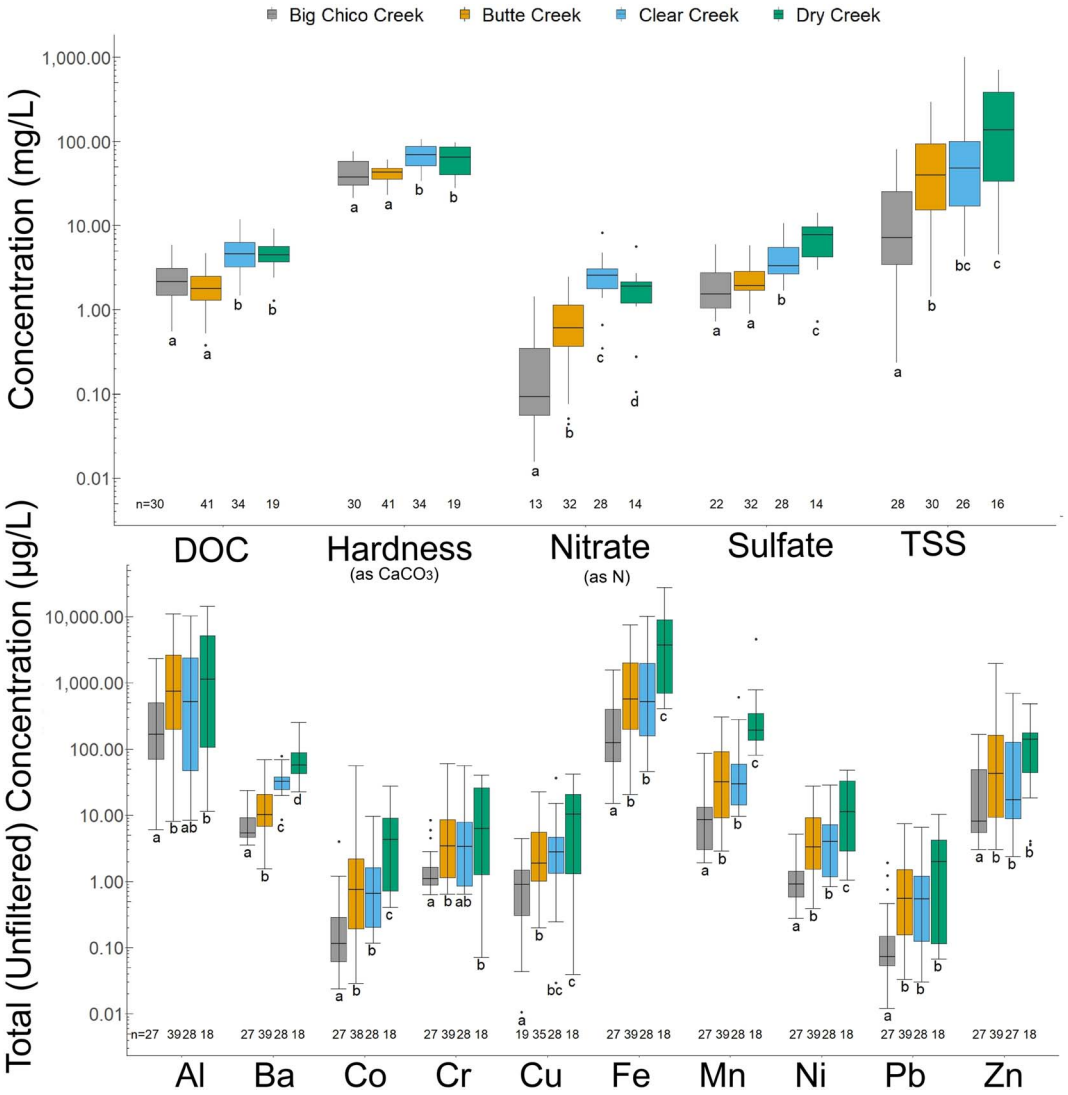


Fig. 4 (a) Box plots of DOC, hardness (as $CaCO_3$), nitrate (as N), sulfate, and TSS in each watershed (mg $L^{-1}$). (b) Box plots of total metal concentrations measured in each watershed (µg $L^{-1}$). Watersheds are displayed in order of increasing number of destroyed structures per urban area. Boxes show 25% and 75% quartiles with the center line at the median of the dataset. The whiskers extend to 5% and 95%, and outliers extend outside of the whiskers. Letters beneath bars show results of Wilcoxon *U* test. Number of samples for each watershed are listed on the bottom of the *y*-axis.

or directly after the hydrograph flow peaks (Fig. S1–S3†). Early precipitation events (November–December 2018) produced lower flows than later precipitation events in January–March 2019 (Fig. 3). However, the early season concentrations of many alkaline and alkaline earth elements were elevated beyond the later season storm flow concentrations (Fig. S1–S7†). Similarly, some of the highest observed Al, Cu, Pb, and Zn concentrations were in the fire-impacted watersheds in December 2018–January 2019. Across nearly all watersheds and flow regimes, total Hg concentrations were near background levels (1–8 ng $L^{-1}$, Table S6†).[44]

### 3.2. Size-fraction analysis of trace and major metals

Total and filter-passing metal concentrations were compared to assess the predominant phase (*i.e.*, particulate *vs.* dissolved) of each metal. After calculating the percent particulate by subtracting the filtered concentration (0.45 µm) from the unfiltered concentration for each sample, the median value for each element was used to group elements according to their predominant phase. Oxide-forming elements, including Al, Fe, Mn, were predominantly measured in the particulate phase (Fig. S8 and S9†). Similarly, most trace metals were predominantly found in the particulate fraction, except for Ba, Cu, and Ni that exhibited a fairly uniform distribution between particulate and filter-passing fractions. Alkaline and alkaline-earth elements (Ca, K, Na, and Mg) were predominantly filter-passing.

Filter-passing metal concentrations (<0.45 µm) were generally higher in burned watersheds when compared to the unburned Big Chico Creek watershed, but differences were not statistically significant ($p > 0.05$) in most cases (Fig. 5). The

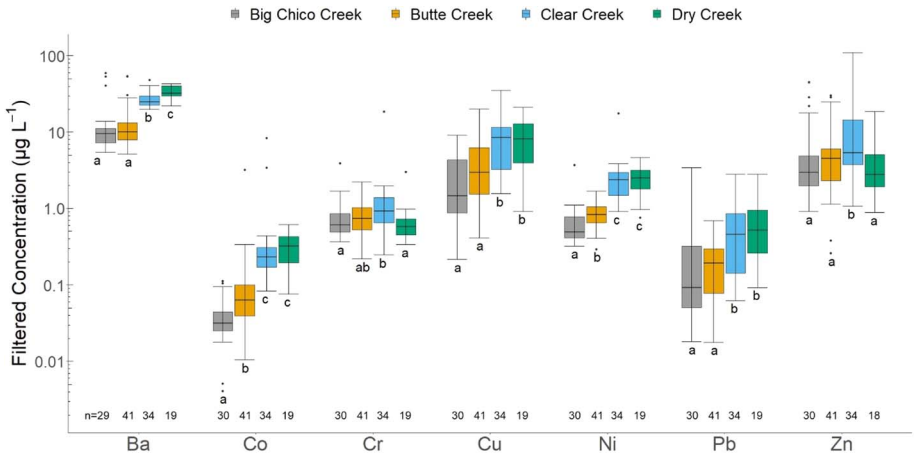


Fig. 5 Box plots of filter-passing metal concentrations measured in each watershed (µg $L^{-1}$). Only metals that have detections for at least 20% of filtered samples are included. Boxes show 25% and 75% quartiles with the center line at the median of the dataset. The whiskers extend to 5% and 95%, and outliers extend outside of the whiskers. Letters beneath bars show results of Wilcoxon *U* test. Number of samples for each watershed are listed on the bottom of the *y*-axis.

exception was Butte Creek, where concentrations of filter-passing Co were statistically greater than in the reference watershed ($p = 1.5 \times 10^{-3}$).

The size fractionation analysis (filter sizes 0.22 µm, 0.45 µm, 0.8 µm, and 1.2 µm) revealed that four elements (*i.e.*, Al, Cr, Fe, and Pb) had statistically higher concentrations (Wilcoxon $U$, $p <$ 0.05, Table S10†) in the 1.2 µm filtrate compared to the 0.22 µm filtrate, suggesting colloidal association (Fig. 6). Al was the only metal with statistically different concentrations between the 0.22 µm and 0.45 µm filter sizes, revealing a slightly wider distribution of colloidal sizes. Comparing median concentrations between filter-size cutoffs to the median total metal concentration informs the proportion of a given metal associated with intermediate colloidal sizes. For the elements with statistically significant differences, the median percentage associated with the 0.22–1.2 µm fraction was 65.6% for Al, 14.3% for Cr, 62.1% for Fe, and 68.6% for Pb. In contrast, no statistically significant difference between filter size cutoffs was observed for Co, Cu, Mn, or Ni, hence most of these elements were either dissolved or associated with the smallest colloidal size fractions.

To summarize, most trace metals were present predominantly as particulates (Fig. S9†), and the only trace metals that did not exhibit a dominant particulate form were Ba, Cu, and Ni. These elements were broadly distributed across phases (Fig. S8 and S9†) and Cu did not exhibit an appreciable colloidal fraction (Fig. 6). Cr and Pb were predominantly (67% or more) found in the particulate fraction using a 0.45 µm filter cutoff (Fig. S9†) and these elements also had measurable colloidal fractions in half of the samples (Fig. 6).

### 3.3. Comparison to historical data

In contrast to many disaster response studies, some historical data exist for hardness in the four burned watersheds and for select trace metals in two burned watersheds.[39] Total median

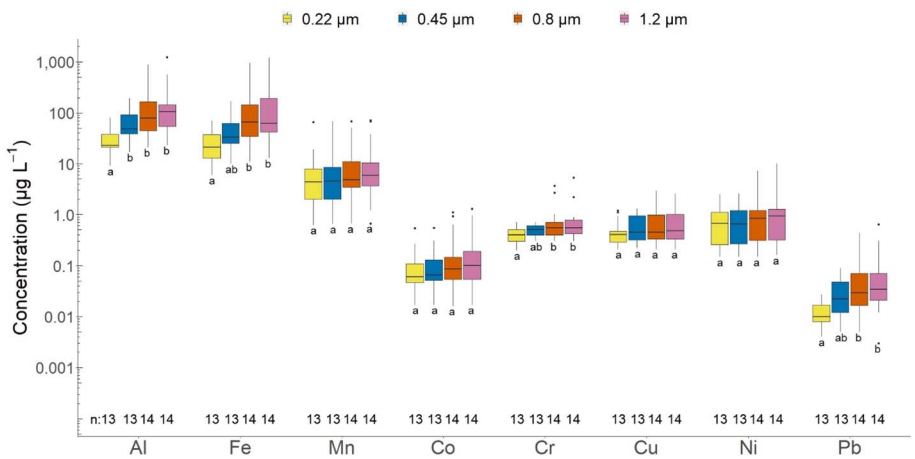


Fig. 6 Box plots of metal concentrations from all watersheds after filtration using pore sizes of 0.22, 0.45, 0.8, and 1.2 µm.[40] Boxes show 25% and 75% quartiles with the center line at the median of the dataset. The whiskers extend to 5% and 95%, and outliers extend outside of the whiskers. Letters beneath bars show results of Wilcoxon *U* test. Number of samples for each filter size are listed on the bottom of the *y*-axis.

 

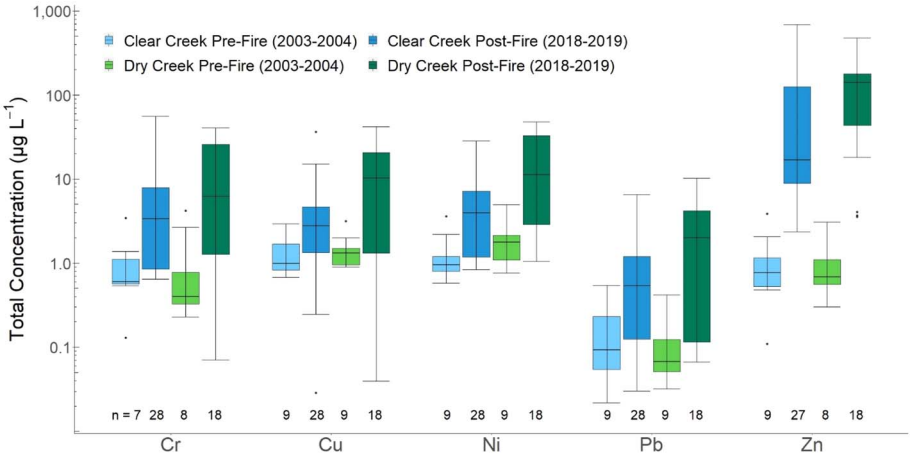


Fig. 7 Total concentration (µg $L^{-1}$) of metals in Clear Creek and Dry Creek before and after the Camp Fire (2018–2019).[39] Boxes show 25% and 75% quartiles with the center line at the median of the dataset. The whiskers extend to 5% and 95%, and outliers extend outside of the whiskers. Number of samples for each watershed are listed on the bottom of the *y*-axis.

concentrations of Cr, Cu, Ni, Pb, and Zn significantly increased in Clear Creek and Dry Creek after the Camp Fire compared to pre-fire concentrations (Fig. 7, Table S12†). The greatest increase was observed for total Zn in both Dry Creek (200-fold) and Clear Creek (22-fold). For Cr and Pb, greater increases were observed in Dry Creek (30- and 22-fold, respectively) compared to Clear Creek (6-fold for both). Cu and Ni concentrations were 3- to 8-fold higher in samples collected after the fire. The pre-fire data were collected through monthly storm sampling from November 2003 to December 2004 in Clear Creek and Dry Creek. Comparing the 2003–2004 and 2018–2019 hydrographs in Butte Creek revealed that storm flow patterns were similar throughout the two years (Fig. S25†).[34]

Comparing annual averages, no statistically significant differences in hardness were found between pre- and post-fire divalent cations in all four watersheds, further supporting the comparability of pre- and post-fire datasets. However, the time-series graphs with data from 2003 to 2004 show consistent hardness concentrations (50–60 mg $L^{-1}$ as $CaCO_3$) throughout the year in Dry Creek and Clear Creek (Fig. S4–S7†). After the fire, hardness was >90 mg $L^{-1}$ as $CaCO_3$ and systematically decreased during the first two months after the fire.

### 3.4. Implications for aquatic health

Metal concentrations were compared to both the EPA acute and chronic aquatic life criteria to assess potential impact on ecosystem health.[45] Only samples with exceedances are discussed in this section (Tables 2, S13†).

The EPA acute aquatic life criteria were exceeded during many sampling events for total Al, Cu, and Zn (Table 2). Total Al exceeded criteria in 51 of 140 samples (36%). Cu exceeded life criteria in 77 cases, with 50 cases for filter-passing samples and 27 cases for total samples. The Zn limit was exceeded in 52 cases, with three cases for filter-passing samples and 49 cases for total samples. For all three elements, the highest number of exceedances occurred in Butte Creek followed by Clear Creek and Dry Creek. Butte Creek had the highest exceedance concentration for both Al at 21 times the limit (February 14, 2019) and Cd at 3.5 times the limit (January 11, 2019). The unburned reference watershed, Big Chico Creek, had fewer exceedances for all elements than the fire-impacted watersheds.

Not only did samples from the urban end-member sites (Paul Byrne Aquatic Park and Little Butte Creek Trailer Park) exceed aquatic life criteria, but the highest concentrations for Cu, Pb, and Zn, were observed at these sites. Samples from Paul Byrne Aquatic Park had the highest acute criteria exceedance concentrations for Cu at 8.4 times the limit, and Pb at 1.5 times the limit, both on May 15, 2019 during a summer storm event. The highest exceedance concentration for Zn was detected at Little Butte Creek Trailer Park on December 18, 2018, at 11 times greater than the acute limit.

The EPA chronic aquatic life criteria concentration limit was exceeded for Al (121 cases), Cd (1), Cu (101), Ni (10), Pb (51), and Zn (50), with the highest exceedance noted for Al (16-fold in Butte Creek, Table 2).

### 3.5. Statistical relationships

**3.5.1. Spearman's rank correlations.** To assess potential sources and transport mechanisms of contaminants, correlations between water quality characteristics were initially assessed using Spearman's rank correlations. Correlations were first calculated with data aggregated across all watersheds (Fig. S10†) and then divided into two subsets to assess if any correlations were unique to burned (Fig. S11†) or unburned (Fig. S12†) watersheds. Correlations for each subset were also calculated for filter-passing (Fig. S13–S15†) and particulate (Fig. S16–S18†) trace metal concentrations. Heat maps in Fig. S10–S18† only report correlation coefficients ($\rho$) for $p < 0.05$.

For total metal concentrations in all watersheds, there were strong positive correlations between all combinations of Al, Ba, Cu, Co, Cr, Fe, Mn, Pb, and TSS ($\rho > 0.42$, Fig. S10†). When comparing burned and unburned watersheds (Fig. S11 and

Table 2 Summary of the number of exceedances of EPA aquatic life criteria peak recommendations (acute and chronic) for each metal and watershed. Total and filter-passing (F-P) fractions are presented. Pb and Ni results are located in Table S13. The no. fold increase is the maximum concentration divided by the limit. A dash (—) is presented when there were no exceedances

| | | | Aquatic habitat recommendation: acute | | | | Aquatic habitat recommendation: chronic | | | |
|---|---|---|---|---|---|---|---|---|---|---|
| Metal | Sample location | Sample type | No. of exceeds | No. fold increase | Max. conc. (ppb) | Limit (ppb) | No. of exceeds | No. fold increase | Max. conc. (ppb) | Limit (ppb) |
| Al | Aquatic Park | Total | 2 | 6.7 | 5000 | 750 | 4 | 58 | 5004 | 87 |
| | Big Chico Creek | F-P | — | — | — | — | 2 | 1.7 | 145 | 87 |
| | | Total | 4 | 3.1 | 2300 | 750 | 19 | 26 | 2304 | 87 |
| | Butte Creek | F-P | — | — | — | — | 9 | 1.8 | 153 | 87 |
| | | Total | 22 | 21 | 15 900 | 750 | 36 | 180 | 15 893 | 87 |
| | Clear Creek | F-P | — | — | — | — | 16 | 6.1 | 528 | 87 |
| | | Total | 13 | 14 | 10 300 | 750 | 19 | 120 | 10 254 | 87 |
| | Dry Creek | Total | 9 | 19 | 14 200 | 750 | 14 | 16 | 14 195 | 87 |
| | Little Butte Creek | F-P | — | — | — | — | 1 | 3.9 | 338 | 87 |
| | Trailer Park | Total | 1 | 3.6 | 2670 | 750 | 1 | 3.1 | 2668 | 87 |
| Cd | Butte Creek | Total | 1 | 3.50 | 2.86 | 0.8 | 1 | 5.8 | 2.86 | 0.49 |
| Cu | Aquatic Park | F-P | 3 | 3.9 | 8.13 | 2.1 | 3 | 3.3 | 8.94 | 2.74 |
| | | Total | 3 | 8.4 | 24.4 | 2.9 | 3 | 8.6 | 24.4 | 2.85 |
| | Big Chico Creek | F-P | 5 | 1.8 | 7.49 | 4.1 | 8 | 2.0 | 7.49 | 3.20 |
| | Butte Creek | Total | 10 | 3.8 | 13.2 | 3.5 | 13 | 3.2 | 22.6 | 7.30 |
| | | F-P | 17 | 4.2 | 20.2 | 4.9 | 24 | 5.5 | 20.2 | 3.65 |
| | Clear Creek | Total | 4 | 3.7 | 36.6 | 8.2 | 5 | 5.3 | 36.6 | 6.88 |
| | | F-P | 14 | 7.3 | 35.5 | 4.9 | 20 | 9.7 | 35.5 | 3.65 |
| | Dry Creek | F-P | 8 | 4.0 | 21.3 | 5.3 | 10 | 5.8 | 21.3 | 3.65 |
| | | Total | 9 | 7.1 | 33.3 | 4.7 | 10 | 65 | 33.3 | 5.16 |
| | Little Butte Creek | Total | 1 | 2.0 | 25.0 | 13 | 1 | 2.5 | 25.0 | 10.1 |
| | Trailer Park | F-P | 2 | 11 | 8.30 | 7.3 | 2 | 16 | 13.4 | 8.18 |
| Zn | Aquatic Park | F-P | 1 | 2.2 | 81.0 | 36 | 1 | 2.2 | 81.0 | 36.5 |
| | | Total | 3 | 7.0 | 258 | 22 | 3 | 11 | 258 | 22.5 |
| | Big Chico Creek | Total | 6 | 3.4 | 166 | 41 | 5 | 4.0 | 166 | 41.6 |
| | Butte Creek | Total | 19 | 52 | 1943 | 69 | 18 | 15 | 1017 | 69.7 |
| | Clear Creek | F-P | 2 | 1.3 | 87.0 | 70 | 2 | 1.2 | 87.0 | 71.3 |
| | | Total | 9 | 14 | 693 | 51 | 9 | 13 | 693 | 51.8 |
| | Dry Creek | Total | 11 | 11 | 478 | 44 | 11 | 11 | 451 | 45.0 |
| | Little Butte Creek Trailer Park | Total | 1 | 1.0 | 1079 | 110 | 1 | 9.8 | 1079 | 110 |

S12†), only Zn showed statistically significant correlations with these same trace elements in burned watersheds and not in the reference watershed Big Chico Creek. Additionally, in the unburned reference watershed, DOC was positively correlated ($\rho$ = 0.42 to 0.65) with TSS, nitrate, and several trace metals (*i.e.*, Al Co, Cu, Fe, Mn). DOC was not correlated with TSS in burned watersheds. In the burned watersheds, nitrate and sulfate were correlated with nearly all constituents.

Considering only filter-passing metals, correlations were calculated for trace metals and other water quality parameters (Fig. S13–S15†). In general, there were more correlations between filter-passing metals and other water quality parameters in the burned watersheds compared to the unburned watershed. Filter-passing Cu was strongly correlated with Pb in both watershed subsets ($\rho$ = 0.81 to 0.89). Between all the trace elements, the number of pairs with significant positive correlations was higher across burned watersheds (31) compared to the unburned watershed (15), where one pair was inversely correlated (Zn *vs.* Fe, $\rho = -0.38$).

For the particulate fraction, correlations were explored for trace elements and other water quality parameters (Fig. S16–S18†). In burned watersheds, all trace metals were positively correlated with one another and with TSS ($\rho$ = 0.44 to 0.96), except for Cu and Zn that had no significant correlation with each other. In the unburned watershed, many of the same pairs were positively correlated except for Ba, Cu, and Zn.

**3.5.2. Principal component analysis (PCA).** Because Spearman correlations are limited to paired comparisons, PCA was used to investigate correlations among groups of water quality parameters simultaneously. PCA was performed using total trace metal concentrations as descriptors for each watershed individually (Fig. S19†) and all watersheds collectively (Fig. S20†). PCA was also performed for all watersheds with water quality parameters (*i.e.*, ionic composition, DOC, TSS *etc.*) as descriptors in combination with total (Fig. 8), filter-passing (Fig. S21†), and particulate (Fig. S22†) trace metal concentrations. For each descriptor, the vector length and direction (rotation) describe the relationship among descriptor and principal components; rotation values for each PCA are reported in Table S14.† The angle between vectors communicates the correlation among descriptors, with a more acute angle representing a higher association.

Correlations within the most abundant, oxide-forming elements (*i.e.*, Al, Fe, Mn) *vs.* within other trace elements were compared (Fig. S10–S12, S16–S18†) because statistical correlations may be indicators of physical transport mechanisms (*e.g.*, adsorption onto oxides). Correlations among oxide-forming elements were watershed specific. For example, Al was strongly correlated with Fe (<5° between vectors) in all watersheds (burned and reference) except for Dry Creek (78°), and Al was only strongly correlated with Mn in Butte Creek (9°). Fe and Mn were not significantly correlated (>10°) in any watershed. Correlations among oxide-forming elements and other trace elements were also watershed specific. Mn was strongly correlated (<10°) with Co and Zn in one burned watershed (Clear Creek) and with Ba, Cu, and Pb in the unburned watershed (Big Chico Creek). In burned watersheds, Al was strongly correlated (<10°) to Cu and Pb in Clear Creek, and Cr and Ni in Dry Creek, but Fe was correlated with Cu (3°) and Pb (5°) in Clear Creek and with Ba in Dry Creek (8°).

PCAs were also performed to examine the relationships among the whole suite of chemical parameters (*i.e.*, trace metals, major cations, pH, DOC, nitrate, and sulfate) across all watersheds for total (Fig. 8), filter-passing (Fig. S21†), and particulate (Fig. S22†) metal concentrations. Describing 65% of the variation, the total metal PCA revealed two major descriptor groupings where all metals (group A) were almost orthogonal to the other water quality parameters (group B) including Ca, K, Mg, Na, DOC, nitrate, sulfate, and pH (Fig. 8). Because trace elements were predominantly in the particulate form (Fig. S9†), these groupings effectively divided descriptors by phase, with group A consisting of particulate constituents and group B representing constituents more likely to be truly dissolved. Vectors for group A were oriented in the negative PC1 direction,

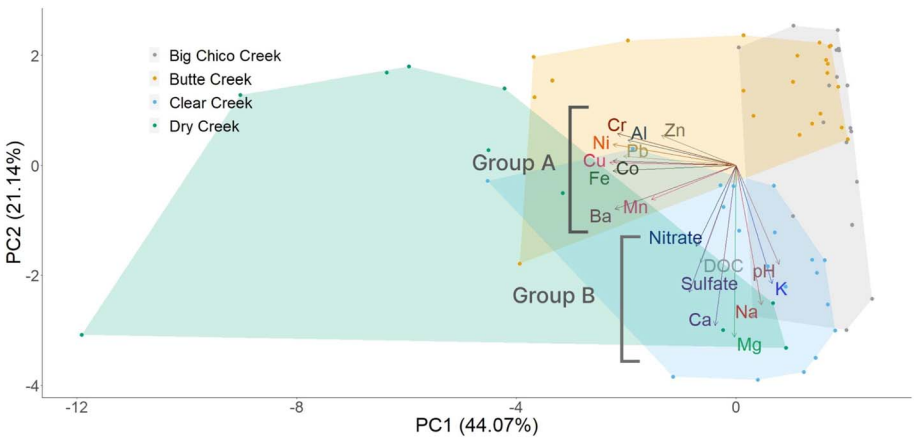


Fig. 8 Principal component analysis (PCA) of all watersheds (Big Chico Creek, Butte Creek, Clear Creek, and Dry Creek) including total trace metal concentrations, major cations, DOC, sulfate, nitrate, and pH. Each point represents a discrete sampling event and shaded areas confine discrete samples within each watershed. Group designations outline two central tendencies of the data, where group A includes trace metals (Al, Ba, Cu, Co, Cr, Fe, Mn, Ni, Pb, and Zn) and group B includes major ions Ca, K, Mg, Na, nitrate, and sulfate, pH, and DOC.

with all vectors pointed away from unburned reference watershed Big Chico Creek. Angles between some pairs of group A vectors showed closer associations with one another compared to group B. For example, several pairs of elements had nearly overlapped vectors, which was not observed in group B.

Although total metal concentration PCAs described >65% of the variance, one limitation of performing PCA with total metal concentrations is that the analysis does not differentiate between filter-passing and particulate concentrations. However, the filter-passing metal PCA explained only 53% of the variance (Fig. S21†), indicating that more components or variables were needed to model the filter-passing metal dataset, which was not interpreted further. Because PCA requires a detected concentration for every element, PCA with particulate metals only included a subset of elements to retain the greatest number of samples in the analysis. The threshold to include an element was that the median value for percent particulate was at least 50% (Fig. S8 and S9†) to minimize excluding samples due to non-detects. The particulate metal PCA (Fig. S22†) explained 84% of variance and showed similar vector relationships to the total concentration PCA (Fig. 8). All vectors were anticorrelated with (pointing away from) the unburned reference watershed (Big Chico Creek). Based on the low percentages of variance explained in several PCAs, and watershed-specific relationships among PCAs, a statistical analysis that uses explanatory variables, such as RDA, is needed to better model water quality (Fig. S22†).

**3.5.3. Redundancy analysis (RDA).** An RDA model revealed that water quality variation (96%) could be modeled by a combination of four explanatory variables: percent of urban land use in each watershed (urban area (%)), number of destroyed structures in each watershed, TSS concentration in each sample, and flow as measured in Butte Creek. Flow was only measured at one location, varying temporally but not spatially among watersheds in this RDA model. The number of destroyed structures and urban area (%) varied spatially by watershed but not temporally. TSS varied both temporally and spatially for each unique sample. The other water quality parameters were used as dependent variables, including total concentrations of trace metals, major cations, major anions, and DOC (Fig. 9). The ESI† includes RDA models for filter-passing (Fig. S23†) and particulate trace metal concentrations (Fig. S24†).

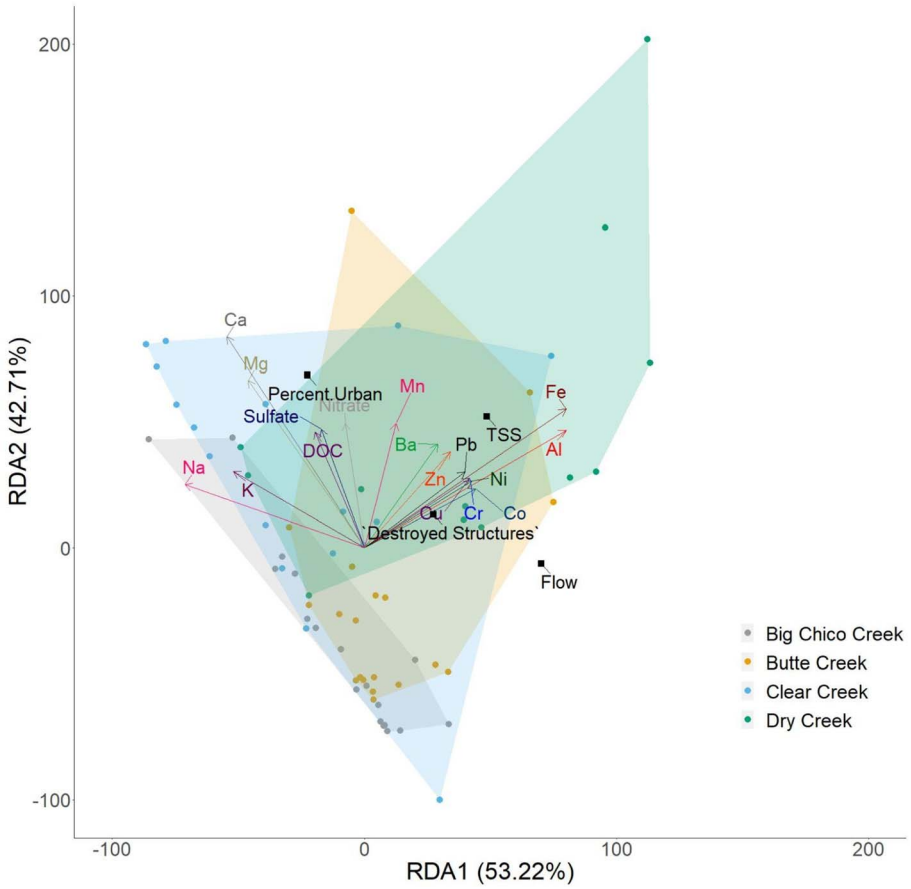


Fig. 9 Redundancy analysis (RDA) of all watersheds (Big Chico Creek, Butte Creek, Clear Creek, and Dry Creek) with dependent variables including total metal concentrations, total major cation concentrations, sulfate, nitrate, and DOC, and independent variables including percent urban land use in watershed, number of burned structures per watershed, TSS, and flow as measured in Butte Creek. Each point represents a discrete sampling event, and shaded areas confine discrete samples within each watershed. RDA was plotted using the scaling I method (correlation biplot).

 

In the RDA analysis, the multidimensional data were reduced to two main axes that represent linear combinations of the explanatory variables. The RDA results provided the coefficients for each explanatory variable in these two axes (Fig. 9), described in eqn (1) and (2). For example, RDA1 increased with flow, TSS, and destroyed structures, and decreased with urban area (%). Comparatively, RDA2 was more sensitive to urban areas (%) (*i.e.*, larger coefficient), less sensitive to destroyed structures, and insensitive to flow. Because the first two axes together explained 96% of variance, additional axes were not interpreted. Each point represents a discrete sample projected onto RDA1 and RDA2 with the shaded areas in Fig. 9, outlining each watershed.

$$\begin{aligned}\text{RDA1} = &(-0.282 \times \text{urban area (\%)}) \\ &+ (0.343 \times \text{destroyed structures}) \\ &+ (0.607 \times \text{TSS}) + (0.878 \times \text{flow})\end{aligned} \quad (1)$$

$$\begin{aligned}\text{RDA2} = &(0.857 \times \text{urban area (\%)}) \\ &+ (0.165 \times \text{destroyed structure}) \\ &+ (0.652 \times \text{TSS}) + (-0.078 \times \text{flow})\end{aligned} \quad (2)$$

Like PCA, the RDA vectors for the water quality parameters are divided into two groups, separating the trace metals (group A) from Ca, K, Mg, Na, DOC, nitrate, sulfate, and pH (group B). The central tendency of each group was approximately orthogonal (*e.g.*, Ca *vs.* Al), similar to Fig. 8 for PCA. However, compared to PCA, the RDA identified some key differences. In PCA, Mn and Ba were strongly correlated (Fig. 8). In the RDA, the correlation between Mn and Ba was weaker, but the correlation between Mn and nitrate was stronger. Lastly, the RDA affirmed strong correlations (<3°) among trace metals and oxide-forming metals, including Cr–Cu, Fe–Cu, Fe–Cr, Cr–Ni, and Al–Ni.

Comparing vectors to the independent variable markers shows the relative association among water quality and the different spatial and temporal explanatory variables (Fig. 9). In the reduced space of the RDA, group A metal vectors aligned most with the number of destroyed structures and TSS. In contrast, three of the group B constituents (sulfate, nitrate, and DOC) aligned with urban area (%). Na and K were differentiated from the other group B constituents and anticorrelated with flow. Fig. 9 also showed that increases in flow corresponded to increases in trace metal concentrations but not increases for major ions or DOC.

RDA was also performed for filter-passing concentrations using only three explanatory variables: urban area (%), number of destroyed structures, and flow. The RDA for filter-passing concentrations explained 99% of the variance (Fig. S23, eqn S2 and S3†). Most of the variance was described by RDA1 (92%), where urban area (%) had the only positive coefficient whereas flow had an almost equal and opposite coefficient. In contrast to Fig. 9, the filter-passing analysis suggested that most trace elements and dissolved group B constituents aligned with urban area (%), not destroyed structures. Found predominantly in the filter-passing fraction, Cu was most closely aligned with the number of destroyed structures, as also seen in Fig. 9. Although predominantly particulate, Zn was observed at appreciable filter-passing concentrations (1–10 μg $L^{-1}$) and its vector nearly bisected the two variables associated with urban wildfire (urban area (%) and destroyed structures). Other close associations in the filter-passing fraction included Pb and Co and Ba and sulfate. All concentrations were anti-correlated with flow along RDA1. With respect to RDA1 and RD2, all water quality vectors were oriented away from the unburned reference watershed Big Chico Creek.

Lastly, an RDA was created for particulate concentrations using the same metals as the particulate PCA (Fig. S24†) with the same explanatory variables as Fig. 9. Over 99% of the variance was explained by RDA1, which is heavily weighted by TSS (eqn S4 and S5†). Only 38 samples had complete data sets (*i.e.*, detects for each element) to perform this RDA.

# 4. Discussion

## 4.1. Metal controls and sources

The primary hypothesis – that widespread urban burning would increase concentrations of metals in storm runoff – was supported by the results of our analysis. Metal concentrations were consistently elevated in burned watersheds compared to the unburned reference watershed (Fig. 4). Compared to available historical data, total concentrations of Cr, Cu, Ni, Pb, and Zn were up to 200-fold higher in Dry and Clear Creeks after the fire (Fig. 7). Previous studies reported that WUI fires increase metal concentrations in surface runoff; however, they did not characterize an event of the magnitude of the 2018 Camp Fire.[17,18,22]

One challenge is attributing the presence of metals in runoff to urban sources (burned or unburned), directly from wildfire, or to historical land uses. For some elements, such as Al, Fe and Mn, it is difficult to ascribe wildland or urban sources, as increases in metals are frequently reported after wildland fires due to enrichment in vegetation ash and subsequent mobilization of ash and underlying soil during runoff events.[5,46]

This study documented significant increases in all metals when comparing the control watershed to the burned watersheds, with higher metals concentrations in watersheds that had more structures destroyed per urban acre. The increased metal concentrations certainly have some dependence on wood ash production. The primary components of wood ash include Ca (13–34%), K (1–13%), Mg (0.1–9%), Al (0.5–1.9%), and Mn (<1%), and Fe (<1%).[46,47] The metals Ca and Mg tend to form carbonate minerals, while Al, Mn, and Fe tend to be in the form of oxides.[46,47] In addition to carbonate minerals and oxides, silicate minerals that include Al, Ca, Fe, K, and Mn can be a component of ash, and the presence of phosphate and sulfate minerals (*e.g.*, apatite, gypsum) have also been reported.[47,48] The observation of increased hardness during early season flushing is explained by the presence of the readily dissolved mineral forms while later season storms with more energy mobilized the oxide forming, less soluble particulates.[49]

The elevated concentrations of trace metals, their strong correlations with one another and with the explanatory variables of the RDA suggest fire-impacted urban areas as likely sources. Trace and major elements (*i.e.*, Ba, Cr, Co, Cu, Fe, Mn,

Ni, Pb, and Zn) most strongly correlated with each other and with the number of destroyed structures and urban area (%). These RDA explanatory variables include urban metal sources, such as automobile components (*e.g.*, frame, mechanical and electrical components, material coatings, and tires) and household and commercial products (*e.g.*, paints, consumer chemicals, electrical wiring, appliances, and electronics).[48,50,51] Storm runoff samples had concentrations of Co, Cr, Mn, Ni, and Pb that were consistently higher than concentrations reported for urban stormwater by a factor of 2–5 (Table 2, Fig. 4), even though the urban density in Paradise, CA was lower than the >90% developed land use in dense urban landscapes.[52] Wood ash is also known to contain some trace metals with toxicity risks that were of interest in this study, such as Cu, Ni, Pb, and Zn. Zn has been reported to be as high as 0.2% of some wood ash, but recent studies conducted in a watershed adjacent to this study have shown that structure and vehicle ashes have a much greater trace metal content than vegetation.[47,48]

Another line of evidence supporting trace elements originating from fire-impacted urban areas is the elevated concentrations observed at the urban end-member locations (Little Butte Creek Trailer Park and Paul Byrne Aquatic Park), which, unlike routine sampling locations in each watershed (Fig. 1), did not receive any dilution from non-urban areas in the watershed. The samples collected at the end-member locations consistently had the highest metal concentrations observed in the study (*e.g.*, Cu > 20 μg $L^{-1}$, Pb > 5 μg $L^{-1}$, and Zn > 1 mg $L^{-1}$, Table 2). Elevated concentrations closer to source materials align with studies reporting that runoff collected from automobile fires can be orders of magnitude higher (*e.g.*, 760–1200 μg $L^{-1}$ Cu, 620–2300 μg $L^{-1}$ Pb, and 8100 to 11 000 μg $L^{-1}$ Zn) than concentrations observed at the end-member locations.[16] It is important to note that the dominant materials of construction at the trailer park are different from other residential construction (*i.e.*, metal *vs.* wood construction, lack of foundations).

Strong consideration was also given to the influence of geological sources including the presence of historical, inactive mines as potential sources for trace elements. Dry Creek has the largest land area impacted by mine tailings (7%) compared to all other watersheds (<0.5%), and the only inactive Mn mines (Table 1). The median Mn concentration in Dry Creek (192 μg $L^{-1}$) was almost an order of magnitude higher than in the other burned watersheds (median: 30 μg $L^{-1}$), which were both higher than in the unburned watershed (median: 9 μg $L^{-1}$, Fig. 4). Although Dry Creek may have a higher likelihood of geologic Mn sources, the urban end-member locations (Little Butte Creek Trailer Park and Paul Byrne Aquatic Park) had appreciable median concentrations (75–117 μg $L^{-1}$) that support burned, urban sources as well. Additionally, Butte Creek was the only watershed with inactive Cr mines (Table 1), but similar Cr concentrations were observed in Clear Creek and higher concentrations were observed in Dry Creek and at the two urban end-member locations. Correlations among Co, Cr, and Ni could indicate leaching from ultramafic soils.[53] However, ultramafic outcrops are not abundant in the study watersheds, suggesting a predominantly anthropogenic source.[53] A similar argument can be made for Ba, which could originate from the Lovejoy basalt that underlies parts of Butte County.[54] However, post-fire concentrations of Ba in fire-affected watersheds were statistically higher than in the reference watershed Big Chico Creek (Fig. 4) which also contacts the Lovejoy Basalt, supporting a likely anthropogenic origin that mobilized from fire-impacted areas.

Total Hg was not found to be from the burned urban environment, and instead all Hg measurements were attributed to historical gold mining activities. Concentrations upstream of the Cherokee mine (1800's era hydraulic mine) were typical for the region, while higher measurements in lower Dry Creek (*e.g.*, peak of 665 ng $L^{-1}$) collected downstream of the mine and the fire can be attributed to a residual mine effect and not a fire effect. Total Hg concentrations measured downstream of the fire were within the ranges of concentrations measured in western slope Sierra Nevada streams.[44] Therefore, although geologic sources cannot be categorically excluded for many of the measured metals, trends among watersheds and concentrations at urban end-member locations support appreciable anthropogenic sources of metals from the burned urban environment, mercury excluded.

A clear distinction emerged from the RDA showing two groups with different transport behavior based on divergent correlations. The trace metals (group A) correlated strongly with TSS and with destroyed structures (Fig. 9), while having less dependence on the urban area (%). These findings potentially indicate the importance of urban burning of houses and vehicles as sources of trace metals in post-fire runoff. The correlation of trace metals with TSS also points to particulate-driven transport for most trace metals. Conversely, the major ions and DOC (group B, Fig. 8) concentrations had a strong negative correlation with flow and a strong positive correlation with urban area (%) (Fig. 9). The emergence of group B points to easily solubilized constituents, such as readily dissolved carbonate minerals of Ca and Mg, base anions, and readily dissolved organic molecules. The correlations of major ions and DOC with urban area may be enhanced due to impervious surfaces increasing the flushing behavior of urban drainages.[55,56] Notably, lower intensity storms immediately after the fire produced lower flows than later storms (Fig. 3), yet generated higher concentrations of Ca, K, and Mg (Fig. S1–S3†). This first flush behavior for hardness was only observed in Dry and Clear Creeks (Fig. S5 and S6†), making it difficult to clearly separate fire and urban effects. These results suggest that the bulk composition of storm runoff highly depends on storm flow energy mobilizing particulates (group A) and the presence of readily dissolved constituents (group B).[49]

### 4.2. Mechanistic analysis

Most trace metals were present predominantly as particulates (Fig. S9†), with the only trace metals that did not exhibit a dominant particulate form being Ba, Cu, and Ni. The total concentrations of metals found predominantly in particulate form (*i.e.*, Al, Cr, Co, Fe, Mn, Pb, and Zn) were strongly correlated with the number of destroyed structures and were weakly

 

and inversely correlated with percent urban development (Fig. 9). While we did not conduct a mineralogical analysis of the samples, we can briefly speculate on the forms and likely associations of metals based on prior studies and chemical equilibrium modeling. For example, correlations among trace metals and the oxide-forming metals Al, Fe, and Mn, and TSS concentrations suggest that trace metal transport is driven by sorption or co-precipitation on more abundant oxide surfaces. The pH values were circumneutral in all streams, which is known to favor the precipitation of Al(III), Mn(IV), and Fe(III) oxides. Modeling of our results using Visual MINTEQ indeed predicted the formation of Al and Fe oxides, and that conditions would favor Co, Cu, Mg, Ni, Pb, and Zn sorption to oxide surfaces.[57]

It is also possible that relationships among oxide-forming metals and trace metals could indicate a shared metal source rather than sorption. Filter-passing Zn concentrations were lower than the method detection limit in 26–74% of samples collected from the mainstem locations but always detected at the urban end-member locations (Table S8†). These differences could indicate that the source and transport of Zn after WUI fires are different from typical watershed weathering processes. For instance, Alshehri *et al.* (2023) found that many metals reported in this study were in nanoparticulate forms within the carbon lattice of ash and co-associated with silicates and carbonate mineral forms.[48] Further, ash derived from structures and vehicles contained Zn-bearing nanoparticles ranging in size from 50 to 450 nm, which overlaps with the size of Zn nanoparticles used in commercial products such as tire rubbers that contain 1–5% of Zn.[48] To date, there is no publicly available estimate of the number of destroyed vehicles by the Camp Fire, but if one assumes one to two vehicles were lost per destroyed structure then the expected number is >20 000 (Table 1) and the rubber in burned tires represents a potential source of particulate Zn.

Beyond sorption mechanisms to the mineral phase, it is also possible that metals react with the organic carbon fraction of ash. Charred biomass could effectively act as a sorbent due to the presence of carboxylic acids, thiols, or amine groups that provide reactive sites within the carbon lattice, like activated carbon or biochar.[58] The particulate organic carbon content of TSS was not measured for this study, but this would be an area of interest for future study.

Trace metal complexation with DOM is also possible, but no correlations were found between DOC and trace metals in this study by Spearman correlation, PCA, or RDA (Fig. S10–S24†). The exception was a correlation between Ba and DOC in burned watersheds, though evidence of strong Ba-complexation by DOM is limited.[59,60] The lack of metal-DOC correlation points away from this mechanism being a driver of metal transport in this particular system and instead suggests metals were particulate-associated.

### 4.3. Consideration of hydrologic conditions

The interpretations of post-fire water quality are acknowledged to be highly dependent on the hydrologic conditions within the watersheds studied. While the mean annual precipitation values are in good agreement between the pre- and post-fire data in the Camp Fire area, timing and magnitude of storms also influence the watershed response and downstream water quality.[61,62] The comparison of Butte Creek hydrographs for the two pre- and post-fire water years clearly shows that the watershed had similar overall streamflow patterns, including similar peak flows, number of storms, and distribution of storms during the year (Fig. S25†).[34] Further, antecedent conditions can greatly influence water quality and watershed responses following periods of wet or dry conditions could cause attribution of water composition changes incorrectly attributed to wildfire.[61–63] While metal concentrations naturally fluctuate with hydrology, mean annual pre- and post-fire water hardness values were statistically indistinguishable in this study. In contrast, post-fire trace and major metal concentrations were found to be up to 200 times higher than the baseline data. The post-fire data clearly indicates an early season flushing effect of hardness metals, but the remaining water-year values are highly consistent with pre-fire concentrations. Together, these factors strongly suggest that elevated concentrations of trace metals post-fire were outside the range of hydrological variability and can be attributed to fire impacts rather than natural concentration fluctuations that would have likely been apparent in hardness metals as well. Further, weather in California has high inter-annual and intra-annual variability, and annual fluctuations in precipitation timing and quantity can be dramatic. Large fluctuations in antecedent watershed conditions make the comparison of water quality data challenging. While acknowledging the possibility of hydrologic influence on metal concentrations, the strong agreement in hardness concentrations pre- and post-fire, while not a perfect comparison, suggests that the overall water quality remained comparable between years, and the large increases in trace metals are likely directly due to the fire perturbation.

### 4.4. Other considerations and limitations

Samples from drainage areas in close geographic proximity were collected in this study. With this side-by-side pairing, there are underlying geologic and vegetation similarities (*e.g.*, conifer forests) compared to other wildfire investigations that are geographically diverse. However, variability did exist for land use type and burn extent. For example, a greater relative area of Clear and Dry Creek watersheds was within the burn area (Fig. 1), and these watersheds had higher urban development. Therefore, the impacts of both fire and urban development would be expected to be amplified in these drainage areas. Although Butte Creek contained the highest number of burned structures, it also had the lowest urban area (%) due to its large, upstream portion that has low development and was unimpacted by fire. Therefore, the observations in Butte Creek may be due to low urban area or the comparatively low fraction of the drainage area that was burned.

Longitudinal sampling within each drainage area could have helped separate some of these confounded effects but was not possible in this study. Sampling was limited to locations on the

lower reaches of each drainage area due to road closures during response and recovery. Another impact of access limitations was that one of the end-member sites (*i.e.*, trailer park) could not be accessed during the earliest sampling events. The burned materials were exposed to several storms before sampling, and concentrations in first flush events may have been higher. First flush data are limited in many wildfire studies due to these logistical constraints.[64] Despite these limitations, this study presents a comprehensive dataset with parallel sites, broad water quality scope, runoff from burned urban areas, and a time-series capturing different hydrologic flow regimes.

## 5. Conclusion

This study found that the wildland–urban interface impacted by the 2018 Camp Fire contributed metals to nearby watersheds at concentrations that could threaten ecosystem health. In addition to elevated concentrations of Mn and Fe commonly observed after wildland fires, urban burning likely contributed elevated concentrations of Al, Ba, Co, Cr, Cu, Ni, Pb, and Zn from anthropogenic fuels such as homes and vehicles.

The transport of metals was likely controlled by land use features (*e.g.*, impervious surfaces in urban environments) and fuel type (*e.g.*, burned structures). Fire-affected creeks draining watersheds with large numbers of burned structures within their urban, impermeable surfaces contained the highest concentrations of trace metals.

Particulate-associated transport emerged as the primary mechanism responsible for the mobilization of metals, possibly attributed to surface interactions with oxide-forming elements or co-formation with ash during combustion throughout the sampling campaign, the mobilization and transport of metals were observed, leading to exceedances of EPA criteria. Peak concentrations of Al, Cd, Cu, Ni, Pb, and Zn surpassed both acute and chronic levels of EPA aquatic habitat criteria, persisting from the immediate aftermath six months after the fire. Consequently, the accumulation of metals in riparian sediment may have adversely impacted ecosystems beyond the duration of surface debris removal efforts. These findings underscore the potential for long-term water quality and ecosystem effects resulting from wildfires in the wildland-urban interface (WUI).

The study highlights the significant contribution of WUI fires to the long-term effects on water quality and ecosystems, as evidenced by the continued mobilization and accumulation of metals even after the fire has subsided and surface debris has been cleared.

## Author contributions

Lauren Magliozzi: investigation, formal analysis, data curation, writing – original draft, writing – review & editing, visualization; Sandrine Matiasek: conceptualization, funding acquisition, project administration, methodology, validation, investigation, formal analysis, data curation, writing – original draft, writing – review & editing; Charles Alpers: conceptualization, funding acquisition, resources, methodology, validation, investigation, formal analysis, data curation, writing – original draft, writing – review & editing; Julie Korak: resources, methodology, validation, data curation, writing – original draft, writing – review & editing; Diane McKnight: supervision, writing – original draft, writing – review & editing; Andrea Foster: formal analysis, writing – original draft, writing – review & editing; Joseph Ryan: supervision, writing – original draft, writing – review & editing; David Roth: resources, writing – review and editing; Peijia Ku: investigation, formal analysis, writing – original draft, writing – review & editing; Martin Tsz-Ki Tsui: resources, investigation, formal analysis, writing – original draft, writing – review & editing; Alex Chow: writing – original draft, writing – review & editing; Jackson Webster: conceptualization, funding acquisition, project administration, methodology, validation, investigation, formal analysis, data curation, writing – original draft, writing – review & editing.

## Conflicts of interest

The authors declare that there are no conflicts of interest.

## Acknowledgements

We would like to acknowledge and thank the editor and anonymous reviewers for their valuable input and help. Additionally, we gratefully acknowledge our many student-helpers Sean Berriman, Eric Dearden, Robert Gruenberg, John Machado, Yovvani Mojica Perez, Jillian Olivar, Erica Plasencia Campos, Dustin Sears, Brice Vanness, Jamie Villatoro, Andrea Villegas-Fregoso, Gabrielle Wyatt for their field assistance and analytical support. We also thank the staff at Chico State Big Chico Creek Ecological Reserve, Radley Ott with Butte County Public Works for assistance with sampling sites access, and Cajun James with Sierra Pacific Industries for lending us autosamplers. This project was funded by NSF RAPID grant CBET-1917165 and by the U. S. Geological Survey Environmental Health Program of the Ecosystems Mission Area. Any use of trade, firm, or product names is for descriptive purposes only and does not imply endorsement by the U.S. Government.

## References

1 NatCatSERVICE, Munich Re, *Natural Catastrophes in 2018*, **https://www.munichre.com/content/dam/munichre/contentlounge/website-pieces/documents/munichre-natural-catastrophes-in-2018.pdf**, (accessed 2022).

2 A. Maranghides, E. D. Link, C. U. Brown, W. Mell, S. Hawks, M. Wilson, W. Brewer, B. Vihnaneck and W. D. Walton, *A Case Study of the Camp Fire – Fire Progression Timeline, Technical Note* 2135, National Institute of Standards and Technology, Gaithersburg, MD, 2021, DOI: **10.6028/NIST.TN.2135**.

3 C. C. Rhoades, J. P. Nunes, U. Silins and S. H. Doerr, The influence of wildfire on water quality and watershed processes: new insights and remaining challenges, *Int. J. Wildland Fire*, 2019, **28**, 721–725, DOI: **10.1071/WFv28n10_FO**.

 

4 L. F. DeBano, *Water Repellent Soils: A State-Of-The-Art*, USDA Forest Service General Technical Report PSW-46, Pacific Southwest Forest and Range Experimental Station, Berkeley, California, USA, 1981.
5 H. G. Smith, G. J. Sheridan, P. N. J. Lane, P. Nyman and S. Haydon, Wildfire effects on water quality in forest catchments: a review with implications for water supply, *J. Hydrol.*, 2011, **396**, 170–192, DOI: 10.1016/j.jhydrol.2010.10.043.
6 M. Parise and S. H. Cannon, Wildfire impacts on the processes that generate debris flows in burned watersheds, *Nat. Hazards*, 2012, **61**, 217–227, DOI: 10.1007/s11069-011-9769-9.
7 A. J. Rust, T. S. Hogue, S. A. Saxe and J. A. McCray, Post-fire water-quality response in the western United States, *Int. J. Wildland Fire*, 2018, **27**, 203–216, DOI: 10.1071/WF17115.
8 J. Abraham, K. Dowling and S. Florentine, Risk of post-fire metal mobilization into surface water resources: a review, *Sci. Total Environ.*, 2017, **599**, 1740–1755, DOI: 10.1016/j.scitotenv.2017.05.096.
9 T. B. Hampton, S. Lin and N. B. Basu, Forest fire effects on stream water quality at continental scales: a meta-analysis, *Environ. Res. Lett.*, 2022, **17**, 064003, DOI: 10.1088/1748-9326/ac6a6c.
10 K. O. Odigie and A. R. Flegal, Pyrogenic remobilization of historic industrial lead depositions, *Environ. Sci. Technol.*, 2011, **45**, 6290–6295, DOI: 10.1021/es200944w.
11 R. E. Wolf, S. A. Morman, P. L. Hageman, T. M. Hoefen and G. S. Plumlee, Simultaneous speciation of arsenic, selenium, and chromium: species stability, sample preservation, and analysis of ash and soil leachates, *Anal. Bioanal. Chem.*, 2011, **401**, 2733–2745, DOI: 10.1007/s00216-011-5275-x.
12 Y. Ma, P. Egodawatta, J. McGree, A. Liu and A. Goonetilleke, Human health risk assessment of heavy metals in urban stormwater, *Sci. Total Environ.*, 2016, **557**, 764–772, DOI: 10.1016/j.scitotenv.2016.03.067.
13 N. R. Jyothi, Heavy metal sources and their effects on human health, in *Heavy Metals: Their Environmental Impacts and Mitigation*, ed. M. Nazal and H. Zhao, IntechOpen, London, UK, 2021, pp. 21–32, DOI: 10.5772/intechopen.91574.
14 V. C. Radeloff, D. P. Helmers, H. A. Kramer, M. H. Mockrin, P. M. Alexandre, A. Bar-Massada, V. Butsic, T. J. Hawbaker, S. Martinuzzi, A. D. Syphard and S. I. Stewart, Rapid growth of the US wildland-urban interface raises wildfire risk, *Proc. Natl. Acad. Sci. U.S.A.*, 2018, **115**, 3314–3319, DOI: 10.1073/pnas.1718850115.
15 G. S. Plumlee, S. A. Morman, G. P. Meeker, T. M. Hoefen, P. L. Hageman and R. E. Wolf, The environmental and medical geochemistry of potentially hazardous materials produced by disasters, in *Treatise on Geochemistry*, ed. H. D. Holland and K. K. Turekian, Elsevier, 2nd edn, 2014, ch. 11.7, pp. 257–304, DOI: 10.1016/B978-0-08-095975-7.00907-4.
16 A. Lönnermark and P. Blomqvist, Emissions from an automobile fire, *Chemosphere*, 2006, **62**, 1043–1056, DOI: 10.1016/j.chemosphere.2005.05.002.
17 E. D. Stein, J. S. Brown, T. S. Hogue, M. P. Burke and A. Kinoshita, Stormwater contaminant loading following southern California wildfires, *Environ. Toxicol. Chem.*, 2012, **31**, 2625–2638, DOI: 10.1002/etc.1994.
18 M. P. Burke, T. S. Hogue, A. M. Kinoshita, J. Barco, C. Wessel and E. D. Stein, Pre- and post-fire pollutant loads in an urban fringe watershed in Southern California, *Environ. Monit. Assess.*, 2013, **185**, 10131–10145, DOI: 10.1007/s10661-013-3318-9.
19 G. S. Plumlee, D. A. Martin, T. Hoefen, R. Kokaly, P. Hageman, A. Eckberg, G. P. Meeker, M. Adams, M. Anthony and P. J. Lamothe, *Preliminary Analytical Results for Ash and Burned Soils from the October 2007 Southern California Wildfires*, U.S. Geological Survey Open-File Report, 2007, vol. 1407, p. 15, DOI: 10.3133/ofr20071407.
20 A. A. Stec, K. Dickens, J. L. J. Barnes and C. Bedford, Environmental contamination following the Grenfell Tower fire, *Chemosphere*, 2019, **226**, 576–586, DOI: 10.1016/j.chemosphere.2019.03.153.
21 G. O. Mendez, *Water-Quality Data from Storm Runoff after the 2007 Fires, San Diego County, California*, U.S. Geological Survey Open-File Report, 2010, vol. 1234, p. 8, https://pubs.er.usgs.gov/publication/ofr20101234.
22 C. A. Burton, T. M. Hoefen, G. S. Plumlee, K. L. Baumberger, A. R. Backlin, E. Gallegos and R. N. Fisher, Trace elements in stormflow, ash, and burned soil following the 2009 Station Fire in southern California, *PLoS One*, 2016, **11**, 1–26, DOI: 10.1371/journal.pone.0153372.
23 J. R. Lead and K. J. Wilkinson, Aquatic colloids and nanoparticles: current knowledge and future trends, *Environ. Chem.*, 2006, **3**, 159–171, DOI: 10.1071/EN06025.
24 G. R. Aiken, H. Hsu-Kim and J. N. Ryan, Influence of dissolved organic matter on the environmental fate of metals, nanoparticles, and colloids, *Environ. Sci. Technol.*, 2011, **45**, 3196–3201, DOI: 10.1021/es103992s.
25 L. Hare, Aquatic insects and trace metals: bioavailability, bioaccumulation, and toxicity, *Crit. Rev. Toxicol.*, 1992, **22**, 327–369, DOI: 10.3109/10408449209146312.
26 H. Blanck, W. Admiraal, R. F. M. J. Cleven, H. Guasch, M. A. G. T. van den Hoop, N. Ivorra, B. Nyström, M. Paulsson, R. P. Petterson, S. Sabater and G. M. J. Tubbing, Variability in zinc tolerance, measured as incorporation of radio-labeled carbon dioxide and thymidine, in periphyton communities sampled from 15 European river stretches, *Arch. Environ. Contam. Toxicol.*, 2003, **44**, 17–29, DOI: 10.1007/s00244-002-1258-4.
27 M. C. Watzin and P. R. Roscigno, The effects of zinc contamination on the recruitment and early survival of benthic invertebrates in an estuary, *Mar. Pollut. Bull.*, 1997, **34**, 443–455, DOI: 10.1016/S0025-326X(96)00132-4.
28 P. R. Paquin, J. W. Gorsuch, S. Apte, G. E. Batley, K. C. Bowles, P. G. C. Campbell, C. G. Delos, D. M. Di Toro, R. L. Dwyer, F. Galvez, R. W. Gensemer, G. G. Goss, C. Hogstrand, C. R. Janssen, J. C. McGeer, R. B. Naddy, R. C. Playle, R. C. Santore, U. Schneider, W. A. Stubblefield, C. M. Wood and K. B. Wu, The biotic ligand model: a historical overview, *Comp. Biochem.*

*Physiol., Part C: Toxicol. Pharmacol.*, 2002, **133**, 3–35, DOI: 10.1016/S1532-0456(02)00112-6.

29 D. W. Burkett and A. E. Conlin, *Soil Survey of Butte Area, California, Parts of Butte and Plumas Counties*, United States Department of Agriculture, Natural Resources Conservation Service, 2006.

30 *California Department of Conservation, Division of Land Resource Protection, Farmland Mapping and Monitoring Program, Butte County Important Farmland, Downloadable Data, 1988–2020*, https://maps.conservation.ca.gov/dlrp/metadata/importantfarmland/butte_meta.htm, (accessed November 2022).

31 *California Department of Forestry and Fire Protection, Camp Fire Structure Status Map*, 2020, https://frap.fire.ca.gov/mapping/gis-data, (accessed November 2022).

32 *California Geological Survey, Geologic Map of California*, 2010, https://www.arcgis.com/home/item.html?id=2a718c86c96e41e298410c8b58515812, (accessed November 2022).

33 *California Department of Conservation, Mines Online (MOL)*, https://maps.conservation.ca.gov/mol/index.html, (accessed November 2022).

34 U.S. Geological Survey, National Water Information System, *USGS Water Data for the Nation*, 2016, DOI: 10.5066/F7P55KJN, https://waterdata.usgs.gov/monitoring-location/11390000/, accessed November 2023.

35 U.S. Geological Survey, *The StreamStats Program*, 2019, https://streamstats.usgs.gov/ss/, (accessed July 2023).

36 *California Department of Water Resources, California Data Exchange Center*, https://cdec.water.ca.gov, (accessed November 2022).

37 P. A. Lydon, Geology and lahars of the Tuscan Formation, northern California, *Mem.–Geol. Soc. Am.*, 1968, **116**, 441–476, DOI: 10.1130/MEM116-p441.

38 U.S. Geological Survey, *Mineral Resources Data System (MRDS)*, https://mrdata.usgs.gov/mrds/, (accessed November 2022).

39 D. L. Brown, *Cherokee Watershed Water Quality Report*, Prepared for Butte County, CA, 2005, p. 84.

40 C. N. Alpers, D. A. Roth, K. D. Scheiderich, J. P. Webster and S. J. Matiasek, *Geochemical Data for Post-Fire Surface Water from Areas Affected by the 2018 Camp Fire, Butte County, California*, USGS Data Release (IP-134247), DOI: 10.5066/P9XOMVMH.

41 R Core Team, *R: A Language and Environment for Statistical Computing (v4.2.1)*, R Foundation for Statistical Computing, Vienna, Austria, 2022, https://www.R-project.org/.

42 B. Schloerke, D. Cook, J. Larmarange, F. Briatte, M. Marbach, E. Thoen, A. Elberg and J. Crowley, *GGally R Package v2.1.2*, https://cran.r-project.org/web/packages/GGally/index.html, (accessed 2021).

43 J. Oksanen, G. L. Simpson, F. G. Blanchet, R. Kindt, P. Legendre, P. R. Minchin, R. B. O'Hara, P. Solymos, M. H. H. Stevens, E. Szoecs, H. Wagner, M. Barbour, M. Bedward, B. Bolker, D. Borcard, G. Carvalho, M. Chirico, M. De Caceres, S. Durand, H. B. A. Evangelista, R. FitzJohn, M. Friendly, B. Furneaux, G. Hannigan, M. O. Hill, L. Lahti, D. McGlinn, M.-H. Ouellette, E. Ribeiro Cunha, T. Smith, A. Stier, C. J. F. Ter Braak and J. Weedon, *vegan R Package v2.6-2*, https://cran.r-project.org/web/packages/vegan/index.html, (accessed October 2022).

44 J. Domagalski, Mercury and methylmercury in water and sediment of the Sacramento River Basin, California, *Appl. Geochem.*, 2001, **16**, 1677–1691, DOI: 10.1016/S0883-2927(01)00068-3.

45 U.S. Environmental Protection Agency, *National Recommended Water Quality Criteria*, https://www.epa.gov/wqc/national-recommended-water-quality-criteria-aquatic-life-criteria-table, (accessed November 2022).

46 M. B. Bodí, D. A. Martin, V. N. Balfour, C. Santín, S. H. Doerr, P. Pereira, A. Cerdà and J. Mataix-Solera, Wildland fire ash: production, composition and eco-hydro-geomorphic effects, *Earth-Sci. Rev.*, 2014, **130**, 103–127, DOI: 10.1016/j.earscirev.2013.12.007.

47 A. Rahman, E. El Hayek, J. M. Blake, R. J. Bixby, A. M. Ali, M. Spilde, A. A. Otieno, K. Miltenberger, C. Ridgeway, K. Artyushkova and V. Atudorei, Metal reactivity in laboratory burned wood from a watershed affected by wildfires, *Environ. Sci. Technol.*, 2018, **52**, 8115–8123, DOI: 10.1021/acs.est.8b00530.

48 T. Alshehri, J. Wang, S. A. Singerling, J. Gigault, J. P. Webster, S. J. Matiasek, C. N. Alpers and M. Baalousha, Wildland-urban interface fire ashes as a major source of incidental nanomaterials, *J. Hazard. Mater.*, 2023, **443**, 130311, DOI: 10.1016/j.jhazmat.2022.130311.

49 R. M. Harrison and S. J. Wilson, The chemical composition of highway drainage waters I. Major ions and selected trace metals, *Sci. Total Environ.*, 1985, **43**, 63–77.

50 H. W. Mielke, C. R. Gonzales, E. Powell, A. Shah and P. W. Mielke, Natural and anthropogenic processes that concentrate Mn in rural and urban environments of the Lower Mississippi River Delta, *Environ. Res.*, 2002, **90**, 157–168, DOI: 10.1006/enrs.2002.4382.

51 J. K. Gietl, R. Lawrence, A. J. Thorpe and R. M. Harrison, Identification of brake wear particles and derivation of a quantitative tracer for brake dust at a major road, *Atmos. Environ.*, 2010, **44**, 141–146, DOI: 10.1016/j.atmosenv.2009.10.016.

52 J. R. Masoner, D. W. Kolpin, I. M. Cozzarelli, L. B. Barber, D. S. Burden, W. T. Foreman, K. J. Forshay, E. T. Furlong, J. F. Groves, M. L. Hladik, M. E. Hopton, J. B. Jaeschke, S. H. Keefe, D. P. Krabbenhoft, R. Lowrance, K. M. Romanok, D. L. Rus, W. R. Selbig, B. H. Williams and P. M. Bradley, Urban stormwater: an overlooked pathway of extensive mixed contaminants to surface and groundwaters in the United States, *Environ. Sci. Technol.*, 2019, **53**, 10070–10081, DOI: 10.1021/acs.est.9b02867.

53 A. M. Stueber and G. G. Goles, Abundances of Na, Mn, Cr, Sc and Co in ultramafic rocks, *Geochim. Cosmochim. Acta*, 1967, **31**, 75–93, DOI: 10.1016/0016-7037(67)90099-3.

54 Q. L. Street, *Regional Paleo-Topographic Setting of the Lovejoy Basalt, Northern California*, MSc thesis, California State

 

University Chico, 2009, https://scholarworks.calstate.edu/concern/theses/6d56zx17z.
55 G. W. Characklis and M. R. Wiesner, Particles, metals, and water quality in runoff from large urban watershed, *J. Environ. Eng.*, 1997, **123**, 753–759.
56 J. J. Sansalone and S. G. Buchberger, Partitioning and first flush of metals in urban roadway storm water, *J. Environ. Eng.*, 1997, **123**, 134–143.
57 J. P. Gustafsson, *Visual MINTEQ Version 3.1 [Computer Software]*, KTH Royal Institute of Technology, 2013, https://vminteq.lwr.kth.se/.
58 H. Li, X. Dong, E. B. da Silva, L. M. de Oliveira, Y. Chen and L. Q. Ma, Mechanisms of metal sorption by biochars: biochar characteristics and modifications, *Chemosphere*, 2017, **178**, 466–478, DOI: 10.1016/j.chemosphere.2017.03.072.
59 V. Cappuyns, Barium (Ba) leaching from soils and certified reference materials, *J. Appl. Geochem.*, 2018, **88**, 68–84, DOI: 10.1016/j.apgeochem.2017.05.002.
60 Y. Yi, M. Xiao, K. M. G. Mostofa, S. Xu and Z. Wang, Spatial variations of trace metals and their complexation behavior with DOM in the water of Dianchi Lake, China, *Int. J. Environ. Res. Public Health*, 2019, **16**, 4919, DOI: 10.3390/ijerph16244919.
61 F. Z. Maina and E. R. Siirila-Woodburn, Watersheds dynamics following wildfires: nonlinear feedbacks and implications on hydrologic responses, *Hydrol. Processes*, 2020, **34**, 33–50, DOI: 10.1002/hyp.13568.
62 F. Z. Maina, E. R. Siirila-Woodburn, M. Newcomer, Z. Xu and C. Steefel, Determining the impact of a severe dry to wet transition on watershed hydrodynamics in California, USA with an integrated hydrologic model, *J. Appl. Hydrol.*, 2020, **580**, 124358, DOI: 10.1016/j.jhydrol.2019.124358.
63 M. E. Newcomer, J. Underwood, S. F. Murphy, C. Ulrich, T. Schram, S. R. Maples, J. Peña, E. R. Siirila-Woodburn, M. Trotta, J. Jasperse and D. Seymour, Prolonged drought in a northern California coastal region suppresses wildfire impacts on hydrology, *Water Resour. Res.*, 2023, **58**, 034206, DOI: 10.1029/2022WR034206.
64 O. D. Raoelison, R. Valenca, A. Lee, S. Karim, J. P. Webster, B. A. Poulin and S. K. Mohanty, Wildfire impacts on surface water quality parameters: cause of data variability and reporting needs, *Environ. Pollut.*, 2023, **317**, 120713, DOI: 10.1016/j.envpol.2022.120713.